Landes Bioscience www.landesbioscience.com

Supplemental Material to:

Anne-Sophie Nicot, Francesca Lo Verso, Francesca Ratti, Fanny Pilot-Storck, Nathalie Streichenberger, Marco Sandri, Laurent Schaeffer, and Evelyne Goillot

Phosphorylation of NBR1 by GSK3 modulates protein aggregation

Autophagy 2014; 10(6)
http://dx.doi.org/10.4161/auto.28479

www.landesbioscience.com/journals/autophagy/article/28479

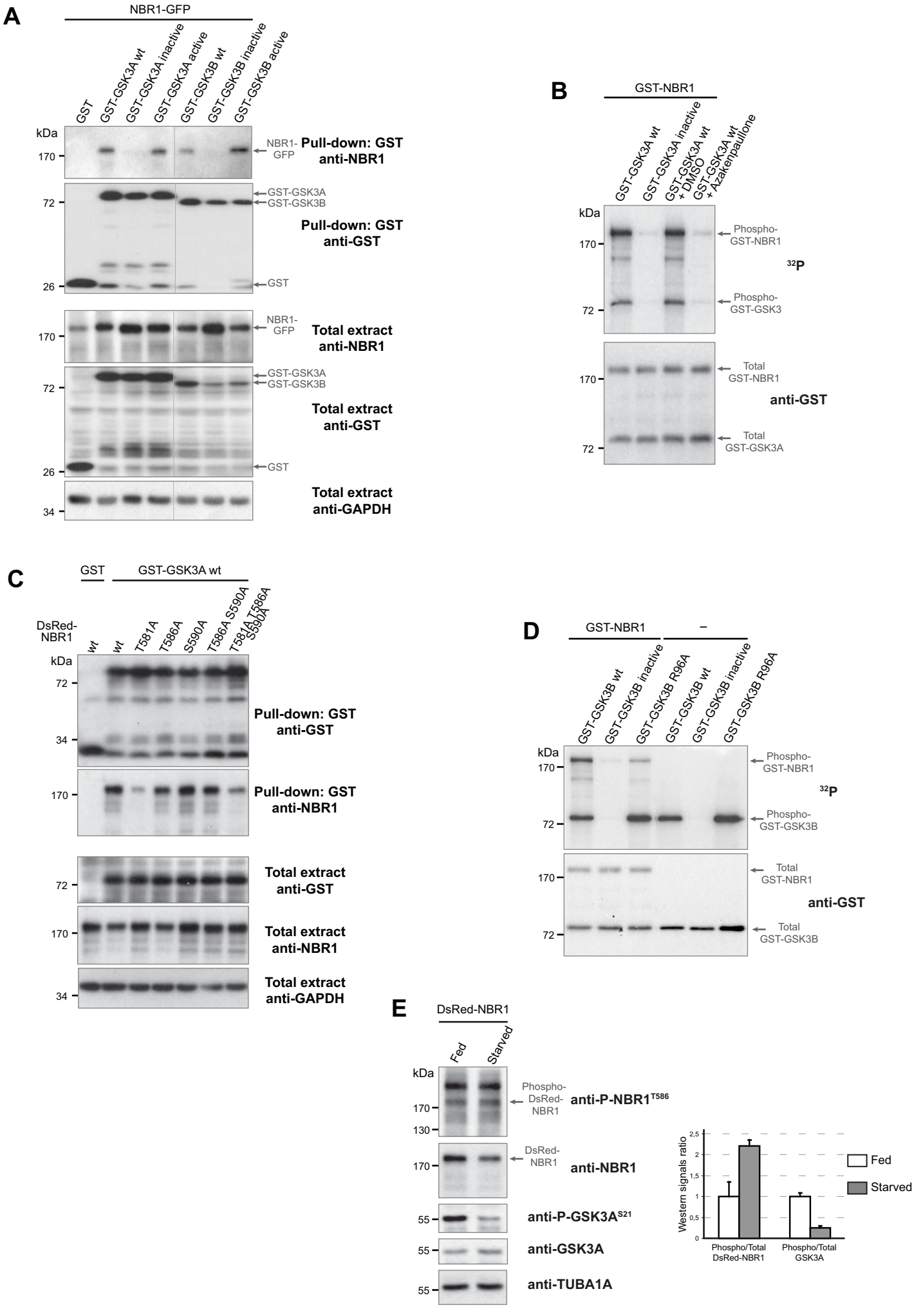
A
NBR1-GFP
GST
GST-GSK3A wt
GST-GSK3A inactive
GST-GSK3A active
GST-GSK3B wt
GST-GSK3B inactive
GST-GSK3B active
kDa
170
72
26
34
NBR1-GFP
GST-GSK3A
GST-GSK3B
GST
Pull-down: GST anti-NBR1
Pull-down: GST anti-GST
Total extract anti-NBR1
Total extract anti-GST
Total extract anti-GAPDH
B
GST-NBR1
GST-GSK3A wt
GST-GSK3A inactive
GST-GSK3A wt + DMSO
GST-GSK3A wt + Azakenpaullone
Phospho-GST-NBR1
32P
Phospho-GST-GSK3
Total GST-NBR1
anti-GST
Total GST-GSK3A
C
GST
GST-GSK3A wt
DsRed-NBR1
wt
T581A
T586A
S590A
T586A S590A
T581A T586A S590A
Pull-down: GST anti-GST
Pull-down: GST anti-NBR1
Total extract anti-GST
Total extract anti-NBR1
Total extract anti-GAPDH
D
GST-NBR1
–
GST-GSK3B wt
GST-GSK3B inactive
GST-GSK3B R96A
Phospho-GST-NBR1
32P
Phospho-GST-GSK3B
Total GST-NBR1
anti-GST
Total GST-GSK3B
E
DsRed-NBR1
Fed
Starved
Phospho-DsRed-NBR1
anti-P-NBR1T586
anti-NBR1
anti-P-GSK3AS21
anti-GSK3A
anti-TUBA1A
Western signals ratio
Phospho/Total DsRed-NBR1
Phospho/Total GSK3A
Fed
Starved

Figure S1

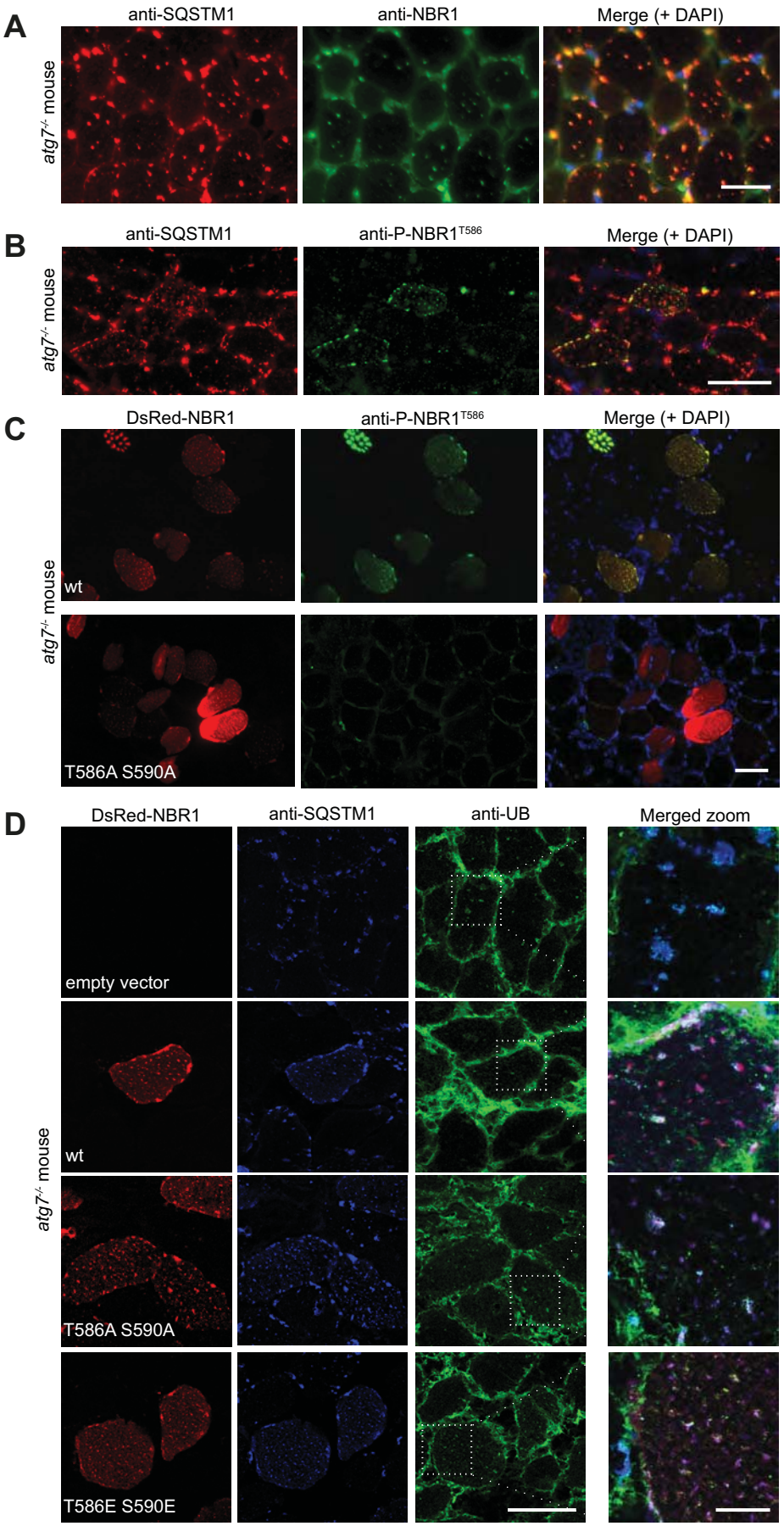
A
anti-SQSTM1
anti-NBR1
Merge (+ DAPI)
atg7-/- mouse
B
anti-SQSTM1
anti-P-NBR1T586
Merge (+ DAPI)
atg7-/- mouse
C
DsRed-NBR1
anti-P-NBR1T586
Merge (+ DAPI)
atg7-/- mouse
wt
T586A S590A
D
DsRed-NBR1
anti-SQSTM1
anti-UB
Merged zoom
atg7-/- mouse
empty vector
wt
T586A S590A
T586E S590E

Figure S2

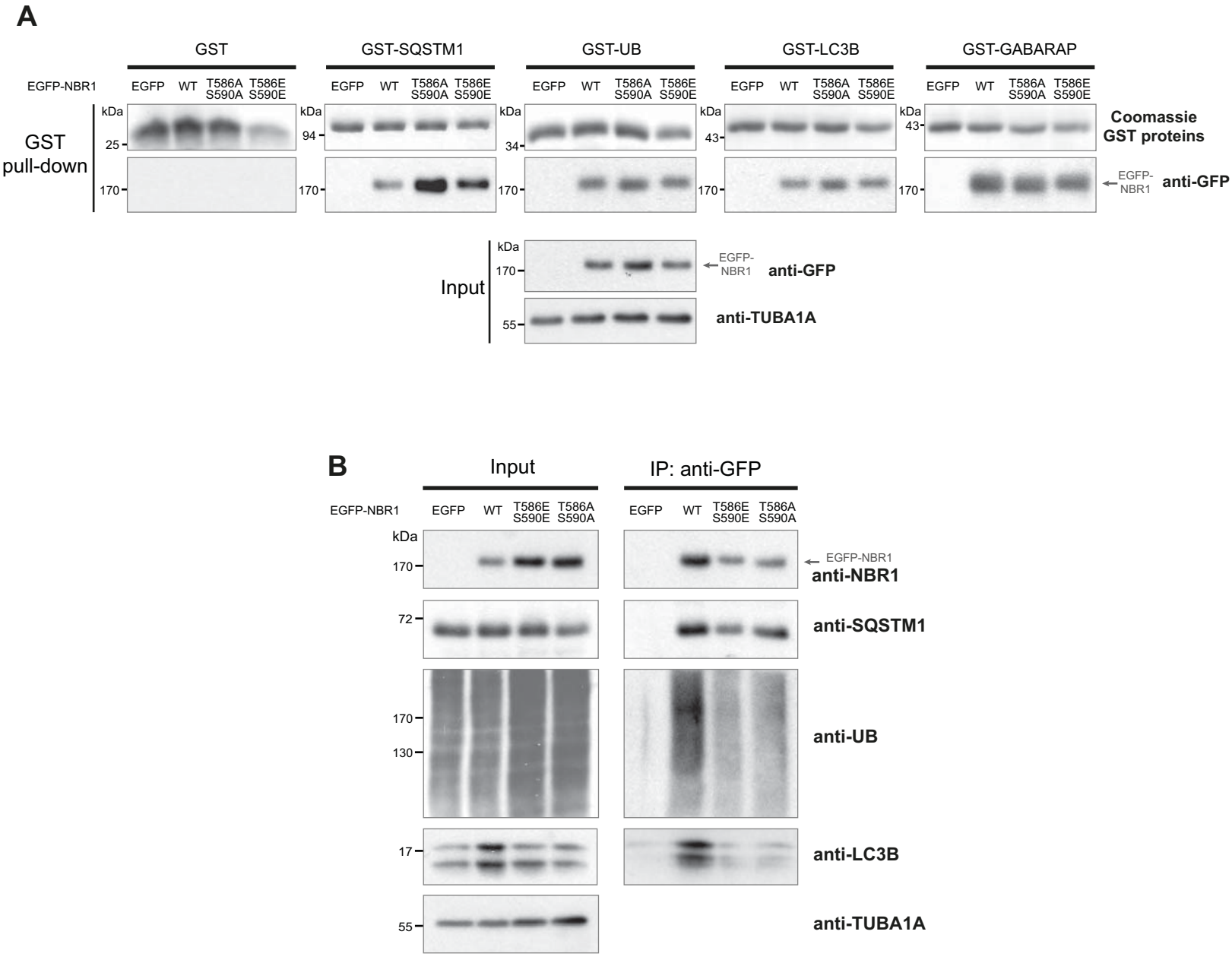
A
GST
GST-SQSTM1
GST-UB
GST-LC3B
GST-GABARAP
EGFP-NBR1
EGFP
WT
T586A S590A
T586E S590E
kDa
GST pull-down
25
94
34
43
170
Coomassie GST proteins
EGFP-NBR1
anti-GFP
Input
55
anti-TUBA1A
B
Input
IP: anti-GFP
anti-NBR1
anti-SQSTM1
130
72
anti-UB
17
anti-LC3B

Figure S3

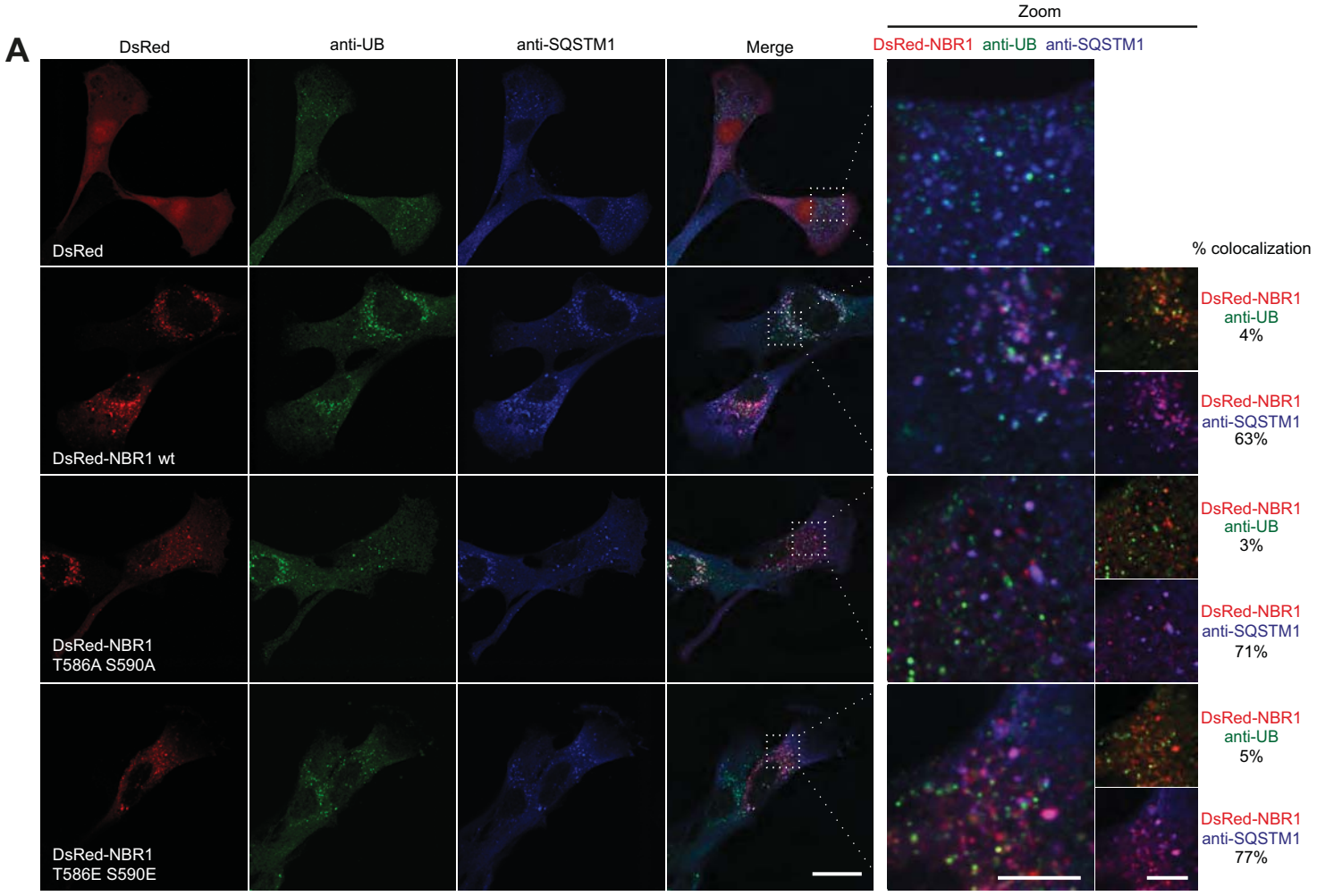
A
DsRed
anti-UB
anti-SQSTM1
Merge
Zoom
DsRed-NBR1 anti-UB anti-SQSTM1
% colocalization
DsRed
DsRed-NBR1 wt
DsRed-NBR1 T586A S590A
DsRed-NBR1 T586E S590E
DsRed-NBR1 anti-UB 4%
DsRed-NBR1 anti-SQSTM1 63%
DsRed-NBR1 anti-UB 3%
DsRed-NBR1 anti-SQSTM1 71%
DsRed-NBR1 anti-UB 5%
DsRed-NBR1 anti-SQSTM1 77%

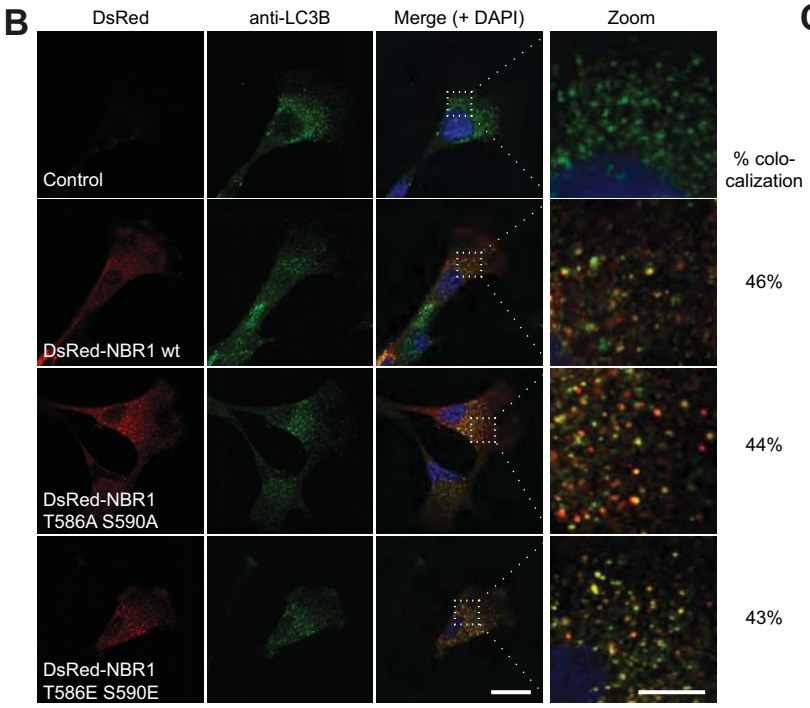
B
DsRed
anti-LC3B
Merge (+ DAPI)
Zoom
% colo-calization
Control
DsRed-NBR1 wt
DsRed-NBR1 T586A S590A
DsRed-NBR1 T586E S590E
46%
44%
43%

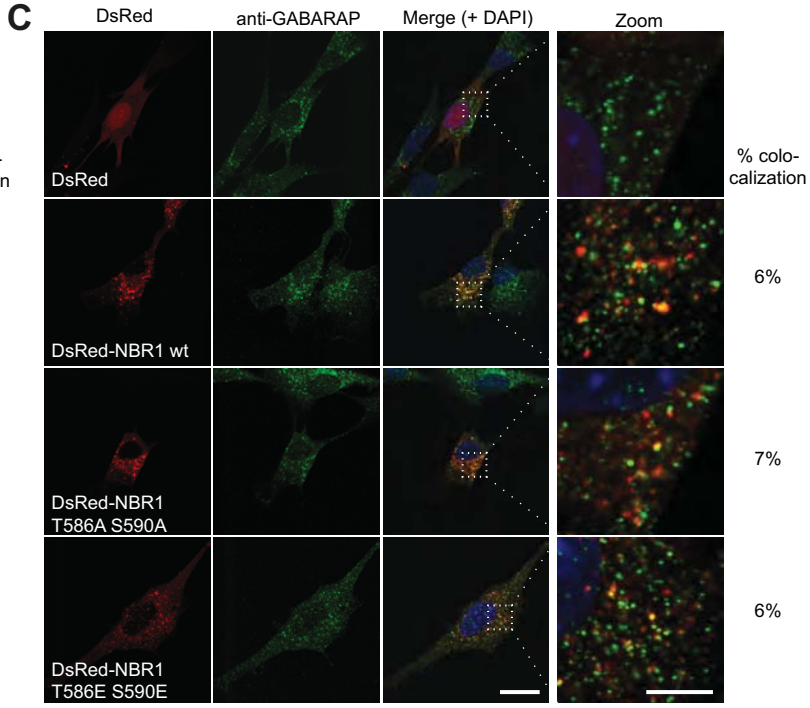
C
DsRed
anti-GABARAP
Merge (+ DAPI)
Zoom
% colo-calization
DsRed
DsRed-NBR1 wt
DsRed-NBR1 T586A S590A
DsRed-NBR1 T586E S590E
6%
7%
6%

Figure S4

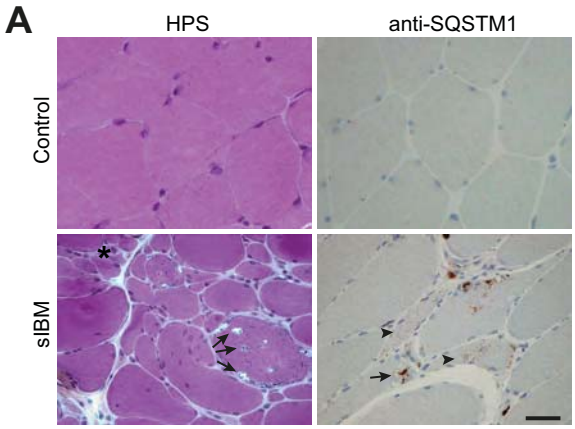
A
HPS
anti-SQSTM1
Control
sIBM
*

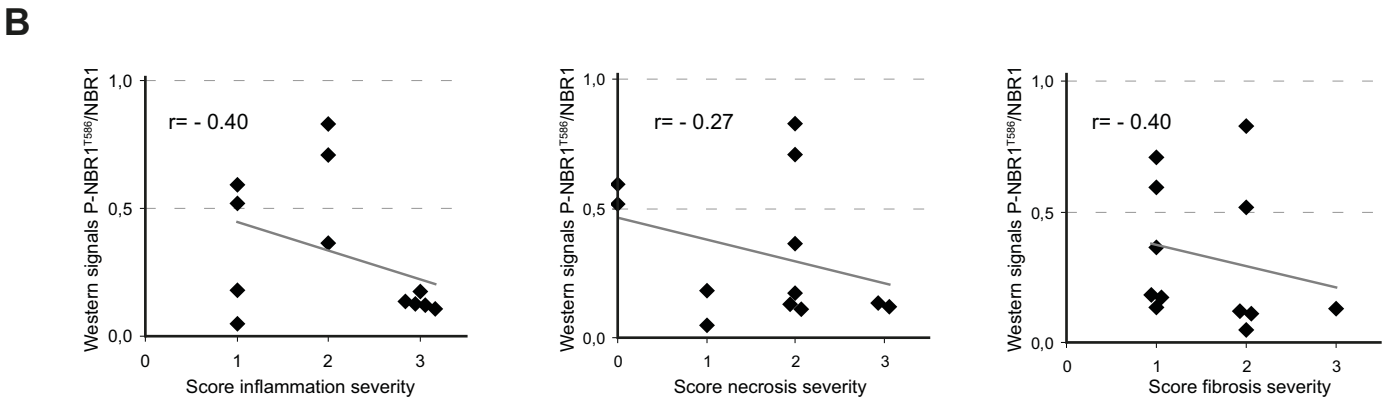
B
Western signals P-NBR1T586/NBR1
1,0
0,5
0,0
r= - 0.40
0
1
2
3
Score inflammation severity
Western signals P-NBR1T586/NBR1
1,0
0,5
0,0
r= - 0.27
0
1
2
3
Score necrosis severity
Western signals P-NBR1T586/NBR1
1,0
0,5
0,0
r= - 0.40
0
1
2
3
Score fibrosis severity

Figure S5

Figure S1. NBR1 binds and is a primed substrate of GSK3. (**A**) Co-affinity purification experiments. GST or GST-tagged GSK3A or GSK3B forms (wt, wild-type; inactive, GSK3A K148A or GSK3B K85A; active, GSK3A S21A or GSK3B S9A) were co-expressed with wild-type GFP-tagged NBR1 in 293T cells. GST-GSK3 were purified and used to affinity isolate NBR1-GFP. (**B**) GSK3 *in vitro* kinase assays performed with wild-type or inactive (K148A) GST-GSK3A mixed with wild-type GST-NBR1. The impact of inactive GSK3A on NBR1 phosphorylation was compared with samples incubated with 1-azakenpaullone, an inhibitor of GSK3 activity, or its solvent DMSO. (**C**) Co-affinity experiments performed with wild-type or nonphosphorylable mutant DsRed-NBR1 affinity isolated by GST or wild-type GST-GSK3A. (**D**) GSK3 *in vitro* kinase assays performed with wild-type GST-GSK3B, inactive (K85A) or R96A mutants mixed with wild-type GST-NBR1. GSK3B R96A is a mutant that cannot phosphorylate primed substrates. (**E**) Western blot showing the level of DsRed-NBR1 phosphorylated on Thr586 and endogenous Ser21-phosphorylated GSK3A in C2C12 myoblasts fed or starved for 2 h. Right panel: ratio of band intensities of phospho- to total DsRed-NBR1, endogenous GSK3A normalized to 1 for the fed condition. Error bars represent standard deviations (n=2).

Figure S2. Total NBR1, SQSTM1 and UB are contained in protein aggregates of *Atg7* muscle-specific knockout mice whereas phospho-NBR1^{T586} is present only in rare fibers with small aggregates. (**A**) Microscopy pictures of muscle transverse sections of *Atg7* muscle-specific knockout mice immunostained for endogenous NBR1 (green) and SQSTM1 (red). Nuclei were stained with DAPI (blue in Merge). Protein aggregates are positive for SQSTM1 and NBR1. Scale bar: 50 μm. (**B**) Muscle transverse sections of *Atg7* muscle-specific knockout mice immunostained for endogenous phospho-NBR1^{T586} (green) and SQSTM1 (red). Nuclei were stained with DAPI (blue in Merge). Phospho-NBR1^{T586} is visible only within fibers containing small SQSTM1-positive aggregates. Scale bar: 50 μm. (**C**) Muscle transverse sections of *Atg7* muscle-specific knockout mice electroporated with wild-type or nonphosphorylable DsRed-NBR1

T586A S590A double mutant (red) immunostained for phospho-NBR1^{T586} (green). Nuclei were stained with DAPI (blue in Merge). Anti-phospho-NBR1^{T586} antibody binds wild-type DsRed-NBR1 but not the nonphosphorylable T586A S590A double mutant. Scale bar: 50 μm. (**D**) Muscle transverse sections of *Atg7* muscle-specific knockout mice electroporated with wild-type DsRed-NBR1 or nonphosphorylable T586A S590A or phosphosphomimetic T586E S590E DsRed-NBR1 double mutant (red) immunostained for SQSTM1 (blue) and UB (FK2 antibody, green). Aggregates and speckles are positive for NBR1, SQSTM1 and UB. Scale bar: 50 μm in left panels, 10 μm in merged zoom.

Figure S3. NBR1 phosphorylation does not modify its physical capacity to interact with autophagy partners LC3B, GABARAP and ubiquitinated proteins, and slightly decreases interaction with SQSTM1. (**A**) GST affinity isolation experiments showing NBR1 interaction with SQSTM1, UB, LC3B or GABARAP. GST-SQSTM1, GST-UB, GST-LC3B or GST-GABARAP were transfected in 293T cells and purified with glutathione beads. Beads were used to affinity isolate EGFP, wild-type EGFP-NBR1, EGFP-NBR1 T586A S590A or EGFP-NBR1 T586E S590E expressed in 293T cells. Inputs and GST affinity isolated products were analyzed by western blot for NBR1 interaction with anti-GFP antibodies and quantities of GST proteins on beads were verified on Coomassie-stained gels. (**B**) EGFP or EGFP-NBR1 forms (wt, wild-type; T586E S590E, phosphomimetic; T586A S590A, nonphosphorylable) were immunoprecipitated from C2C12 myoblasts with anti-GFP antibody. Coimmunoprecipitations of endogenous SQSTM1, ubiquitinated proteins and LC3B were verified. Quantities of coimmunoprecipitated ubiquitinated proteins and LC3B correlate with the levels of EGFP-NBR1 forms present on beads. A slightly higher amount of SQSTM1 was coimmunoprecipitated with EGFP-NBR1 T586A S590A as compared to EGFP-NBR1 T586E S590E.

Figure S4. NBR1 phosphorylation does not modify its colocalizations with SQSTM1, UB, LC3B and GABARAP. Confocal microscopy pictures of C2C12 myoblasts transfected with DsRed empty plasmid, wild-type DsRed-NBR1, DsRed-NBR1 nonphosphorylable (T586A S590A) or phosphomimetic (T586E S590E) mutants. Cells were immunostained for endogenous UB and SQSTM1 (**A**), LC3B (**B**) or GABARAP (**C**). In (**B**), diffuse control DsRed was lost by the methanol immunostaining procedure. The percentage of dots positive for both proteins tested is depicted on the right of the enlargements. Scale bars: 20 μm in left panels, 5 μm in zoom.

Figure S5. No correlation exists between the level of phospho-NBR1^{T586} and the severity of inflammation, necrosis or fibrosis in muscles of sIBM patients. (**A**) Left pictures: Haemalum phloxin saffron (HPS)-stained frozen sections of muscle biopsies from control and sIBM patients. sIBM patient muscle displays atrophied fibers, necrotic fibers (star), fibrosis (pale pink in intercellular space) and numerous rimmed vacuoles (arrows) in muscle fibers. Right pictures: immunostaining of frozen muscle sections with anti-SQSTM1 antibody. sIBM muscle shows SQSTM1-positive aggregates in a rimmed vacuole (arrow) and in the cytoplasm (arrowheads) within muscle fiber. Scale bar: 20 μm. (**B**) Anti-P-NBR1^{T586}/anti-NBR1 signals of each sIBM patient determined by western blot in Figure 5 represented as a function of severity scores for different muscular symptoms: inflammation, necrosis, fibrosis (cf **Table S1**). In gray is the trend line. r= Spearman rho correlation coefficient. $p > 0.05$: there is no significant association between the level of phospho-NBR1^{T586} and the severity of inflammation, necrosis or fibrosis in sIBM muscles.

Table S1. Clinical data and severity scores of sIBM patients

Patients	Sexe	Age (years)	Muscle weakness	Onset of symptoms	Muscle biopsy	CPK (µg/L)	Severity scores				Western: signal ratio P-NBR1^{T586}/NBR1
							Protein aggregation	Inflammation	Necrosis	Fibrosis	
IBM 1	Male	60	Lower limbs	3 years	Left quadriceps	1000	3	3	2	3	0.128
IBM 2	Male	46	Lower limbs	2 years	Right quadriceps	800	2	1	0	1	0.593
IBM 3	Male	67	Lower limbs	Several years	Right quadriceps	1300	3	3	3	2	0.120
IBM 4	Male	77	Lower limbs	2 years	Left quadriceps	100	3	1	1	2	0.050
IBM 5	Male	52	Lower limbs	5 years	Left quadriceps	?	1	1	0	2	0.518
IBM 6	Female	62	Lower limbs	5 years	Left tibialis anterior	333	1	1	1	1	0.181
IBM 7	Male	65	Lower + upper limbs	4 years	Left biceps	1500	2	2	2	1	0.364
IBM 8	Female	64	Quadriceps	Progressive onset	Right quadriceps	900	2	3	2	1	0.174
IBM 9	Female	66	Lower limbs	7 years	Left quadriceps	440	2	2	2	2	1.515 *
IBM 10	Female	82	Lower limbs	7 years	Right quadriceps	300	2	3	2	2	0.109
IBM 11	Male	64	Lower + upper limbs	3 years	Left biceps	359	0	2	2	1	0.707
IBM 12	Female	67	Quadriceps	?	?	1000	2	2	2	2	0.828
IBM 13	Male	60	Lower limbs	2 years	Right quadriceps	540	3	3	3	1	0.134

* Extreme value excluded by Grubbs test at 5%.

CPK = Creatine phosphokinase. Readout of muscle damage (normal value: 10 -120 µg/L)

Table S2. Sequences of primers and siRNA oligonucleotides

Primer name	Forward primer	Reverse primer	Use
		Cloning	
Hs*NBR1*-pENTR1A	GCCGCCGGTACCTCACCATGGAACCACAGGTTACTC	CCGCCGCTCGAGTCTCAATAGCGTTGGCTGTAC	Cloning of Hs *NBR1* into pENTR1A by restriction KpnI/XhoI
Hs*SQSTM1*-pENTR1A	GCCGCCGGTACCTCACCATGGCGTCGCTCACCGTG	CCGCCGCTCGAGTCTCACAACGGCGGGGGATGC	Cloning of Hs *SQSTM1* into pENTR1A by restriction KpnI/XhoI
Hs*LC3B*-pENTR1A	GCCGCCGGTACCTCACCATGCCGTCGGAGAAGACC	CCGCCGCTCGAGTCTTACACTGACAATTTCATCCCG	Cloning Hs *LC3B* into pENTR1A by restriction KpnI/XhoI
Hs*UB*-pENTR1A	GCCGCCGGTACCTCACCATGCAGATTTTCGTGAAAACCC	AATATTGCGGCCGCTCTCAACCACCACGAAGTCTC	Cloning of Hs *UB* into pENTR1A by restriction KpnI/NotI
		Mutagenesis (mutated residues are underlined)	
HsNBR1-T581A	GAGAGTGCCCCACAACGCTCCTGTGGATGTGACTC	GAGTCACATCCACAGGAGCGTTGTGGGGCACTCTC	Mutagenesis of HsNBR1 wt in T581A
HsNBR1-T586A	CCTGTGGATGTGGCTCCCTGCATGTCTCCTC	GAGGAGACATGCAGGGAGCCACATCCACAGG	Mutagenesis of HsNBR1 wt in T586A & T581A in T581A/T586A
HsNBR1-S590A	CTCCCTGCATGGCTCCTCTGCCACATGACAG	CTGTCATGTGGCAGAGGAGCCATGCAGGGAG	Mutagenesis of HsNBR1 wt in S590A & T586A in T586A/S590A & T581A/T586A in T581A/T586A/S590A
HsNBR1-T586E	CTGTGGATGTGGAGCCCTGCATGTC	GACATGCAGGGCTCCACATCCACAG	Mutagenesis of HsNBR1 wt in T586E
HsNBR1-T586E/S590E	GAGCCCTGCATGGAACCTCTGCCACATGAC	GTCATGTGGCAGAGGTTCCATGCAGGGCTC	Mutagenesis of HsNBR1 T586E in T586E/S590E
HsGSK3B-R96A	GACAAGAGATTTAAGAATGCAGAGCTCCAGATCATGAG	CTCATGATCTGGAGCTCTGCATTCTTAAATCTCTTGTC	Mutagenesis of HsGSK3B wt in R96A
		siRNA	
siRNA Hs *NBR1*	AAACCUGACUUUGGCUUCCACAGAA	UUCUGUGGAAGCCAAAGUCAGGUUU	siRNA Hs *NBR1*
siRNA Mm *Nbr1* (#MSS206945, Life Technologies)	CCCUUGUGGACAGUGUGAGUCAUCA	UGAUGACUCACACUGUCCACAAGGG	siRNA Mm *Nbr1*